Engineering Science and Technology, an International Journal 22 (2019) 827–839

HOSTED BY

Contents lists available at ScienceDirect

Engineering Science and Technology, an International Journal

journal homepage: www.elsevier.com/locate/jestch

Full Length Article

Enhancing voltage stability and LVRT capability of a wind-integrated power system using a fuzzy-based SVC

Hamid Rezaie [a,*], Mohammad Hossein Kazemi-Rahbar [b]

[a] Deptartment of Electrical Engineering, Amirkabir University of Technology, Tehran, Iran
[b] Deptartment of Electrical Engineering, Shahed University, Tehran, Iran

ARTICLE INFO

Article history:
Received 29 September 2018
Revised 11 November 2018
Accepted 29 December 2018
Available online 8 January 2019

Keywords:
Voltage stability
Low voltage ride through
Wind power
Static var compensator
Fuzzy control

ABSTRACT

The static var compensator (SVC) has widespread applications in voltage regulation and stability improvement of power systems. This paper studies the SVC performance in a single machine (doubly-fed induction generator (DFIG) employed in a wind farm) infinite bus (SMIB) system. The SVC is employed to improve the voltage stability of the system and the low voltage ride-through (LVRT) capability of the wind farm. To enhance the effectiveness of the SVC, a supplementary fuzzy-based controller (FC) is proposed and is integrated into the SVC controller. The use of the proposed FC leads to the increasing the accuracy of the SVC controller that results in improving its performance in both transient and steady state. By using the proposed controller, the steady state voltage is enhanced and the maximum voltage drop under fault situations is decreased. Less voltage drop after the fault occurrence using the proposed FC results in improving the LVRT capability and makes the wind farm able to meet the grid code requirements in a larger range of load variations in the system. Using extensive simulations in MATLAB/Simulink, the effectiveness of the proposed method in improving the voltage stability and LVRT capability is validated and its effects on the performance of the DFIG-based wind turbine are studied. Three different cases are investigated in the system simulation, in which by using the proposed FC, the steady state voltage error at the load bus and the maximum voltage drop after the fault occurrence at the generator (wind farm) bus are decreased by 74.44% and 25.16% on average, respectively.
© 2018 Karabuk University. Publishing services by Elsevier B.V. This is an open access article under the CC BY-NC-ND license (http://creativecommons.org/licenses/by-nc-nd/4.0/).

1. Introduction

In recent years, the global warming issue has become one of the main human concerns. To tackle this problem, significant efforts have been devoted to reducing the amount of greenhouse gas emissions caused by electricity generation from fossil fuels. For this purpose, besides considering the pollutant emissions in generation scheduling [1], increasing the penetration of renewable energy resources (RERs) into power systems is among the most effective strategies. However, due to the intermittent nature of a majority of RERs, the increment in their penetration can cause serious challenges in power systems in terms of stability and reliability. In this regard, many research works have been conducted to deal with these challenges through proper scheduling and controlling the power systems integrated with RERs, such as [2–6].

Wind energy is among the fastest growing RERs, so its stability, reliability, and safety have been significant in recent years. There are several technical specifications known as "grid codes" for connecting electrical energy sources to the electric network. The grid code requirements (GCRs) for wind generations, define specifications to stabilize wind generations and make them behave like conventional power plants. Wind generations should be able to satisfy these requirements when connecting to the network [7,8].

GCRs consist of two sections: a) static and b) dynamic. The static section reviews the steady state performance of the system like frequency and voltage regulation, and reactive and active power control. The dynamic section is related to the system performance under fault situations and disturbances. The most important subject reviewed in the dynamic section of grid codes with respect to the wind power is the low voltage ride-through (LVRT) capability.

Previously, wind farms like other distributed generations (DGs) were allowed to disconnect from the network during fault situations. Recently, due to the increasing the wind generations, disconnecting wind farms from the network during fault periods can cause more voltage drops and increase the risk of voltage collapse [9]. In this regard, in several modern countries, the system operators have revised their GCRs by determining an operational

* Corresponding author.
E-mail address: h.rezaie@aut.ac.ir (H. Rezaie).
Peer review under responsibility of Karabuk University.

https://doi.org/10.1016/j.jestch.2018.12.018
2215-0986/© 2018 Karabuk University. Publishing services by Elsevier B.V.
This is an open access article under the CC BY-NC-ND license (http://creativecommons.org/licenses/by-nc-nd/4.0/).

behavior for wind farms, which has several control tasks similar to what is defined for conventional generation units. The fault ride-through (FRT) capability of wind farms is one of those control tasks, according to which the wind-turbine generators (WTGs) should remain connected to the grid during fault situations and have the LVRT capability. They specify LVRT characteristics that clearly define the voltage levels and their duration under the fault situation, in which WTGs should remain connected to the network. Further information on this subject can be found in [10] that presents a nonlinear dynamic model of FRT capability of DFIG-based wind farms followed by detailed corresponding simulations and discussions. Fig. 1 shows a typical LVRT characteristic. Considering the amount of wind power generation and the network stability, the GCRs for LVRT are various in different countries. Table 1 gives the LVRT characteristics in several countries [11].

A concise review of the exciting methods for improving the LVRT performance of wind farms is presented in [12]. In addition to the techniques reviewed in this paper, over the last decade, the use of the flexible alternating current transmission system (FACTS) devices and energy storage systems (ESSs) such as flywheel, supercapacitor, and batteries to enhance the LVRT capability of wind farms has attracted a lot of attention. For instance, in [13], the LVRT capability enhancement is studied by placing a static synchronous compensator (STATCOM)-supercapacitor system at the bus to which the DFIG-based wind farm is connected, and in [14], a supercapacitor type ESS is employed at the DC-link of the DFIG for this purpose. It is worth mentioning that ESSs have also widespread applications in the power control of WTGs [15–17].

In this paper, the LVRT capability is enhanced by proposing a new fuzzy-based controller for a static var compensator (SVC) employed to enhance the voltage stability. SVC is among the shunt-connected types of FACTS devices and plays important roles in both stability improvement and voltage regulation in power systems [18]. SVC can control the voltage profile by sufficient absorption or injection of reactive power. Each static var system consists

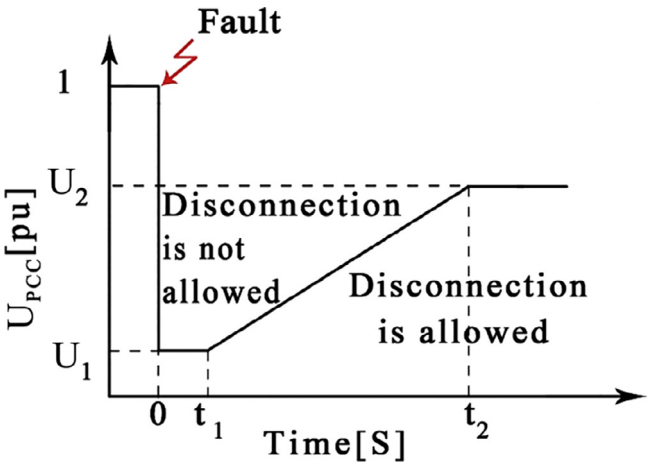

Fig. 1. A typical LVRT characteristic.

Table 1
LVRT characteristics in different countries.

Country	Lowest voltage (U_1)	t_1 (msec)	t_2 (msec)	Final voltage (U_2)
Denmark	20	100	750	75
USA	15	625	3000	90
England	15	150	1200	80
Italy	20	500	800	75
Spain	20	500	1000	80

of one or several basic types of reactive power control elements. These elements include thyristor-switched capacitor (TSC), thyristor-controlled reactor (TCR), thyristor-switched reactor (TSR), saturated reactor (SR), thyristor-controlled transformer (TCT), self-commutated converter (SCC), and line-commutated converter (LCC) [19].

To improve the SVC performance, its conventional control system has been modified using intelligent systems in several previous research works such as [20–28]. In [22], a fuzzy-based controller (FC) is employed to increase the effectiveness of the SVC. The FC is added to the conventional control system of the SVC to achieve the inter-area oscillation damping and transient stability improvement. In [25], an adaptive fuzzy logic controller has been added to the SVC controller, which is designed based on the oscillation energy descent strategy to enhance the system stability in the transient state. In [26], the SVC performance is studied in a power system with wind turbines. In this work, an auxiliary control signal generated by an adaptive network-based fuzzy inference system (ANFIS) is added to the controller to enhance the stability of the system. In [27], an SVC composite controller is designed based on the ANFIS architecture. The control technique suggested in this work enables the SVC to control the voltage collapse and chaotic oscillations of the power system. It is worth mentioning that the use of the ANFIS architecture in methods suggested in [26,27] makes their implementation more complicated than other intelligent control techniques suggested and designed based on pure fuzzy systems.

This paper investigates the SVC performance in a single machine infinite bus (SMIB) system with a DFIG-based wind farm. The SVC unit employed in this study consists of three TSC parts and one TCR part and is used for improving the voltage stability of the system as well as enhancing the LVRT capability of the wind farm. To enhance the SVC performance, a new FC is proposed and is integrated into the SVC controller that improves its accuracy and performance in both transient and steady state. Thereby, employing the proposed FC in the SVC control system leads to the improving the voltage stability of the system by decreasing the steady state voltage error and increasing the system capability to maintain the voltage magnitude in the acceptable range despite the load variations. It also enhances the transient behavior of the system by improving the SVC response to the system disturbances that results in decreasing the maximum voltage drop after the fault occurrence. Therefore, the use of the proposed FC in the SVC controller enhances its effectiveness in improving the LVRT capability of the wind farm and increases the system capability to meet the GCRs in a larger range of load variations. Furthermore, the proposed control technique has shown suitable side effects on the performance of the DFIG-based wind turbine. Moreover, in this paper, in addition to the explaining the design procedure of the proposed FC, it is tried to provide beneficial information about the fuzzy logic concept and applications, its pros and cons, and the generalized design procedure of a fuzzy controller.

The organization of the rest of this paper is as follow:

Section 2 presents the overall system modeling, and in Section 3, the proposed FC design is explained. In Section 4, the effectiveness of the suggested technique to improve the steady state voltage and enhance the LVRT capability is verified using system simulation in Simulink software. Section 5 provides conceptual discussions regarding fuzzy controllers and some suggestions for future works.

2. System modeling

The model of a SMIB system is described in Section 2.1, in Section 2.2, the principles of the SVC operation are discussed, and a dynamic model for DFIG is presented in Section 2.3.

2.1. SMIB system

A simple schematic of a SMIB system is represented in Fig. 2, which includes one generator bus, one infinite bus, two transmission lines, and one load bus. The basic equations of the generator model are as follow:

$$\dot{\delta}_m = \Delta\omega \tag{1}$$

$$\Delta\dot{\omega} = \frac{1}{M}(T_m - T_e - D\Delta\omega) \tag{2}$$

where δ_m, $\Delta\omega$, M, T_m, T_e and D are power angle, rotor speed deviation, inertia constant, mechanical torque, electrical torque and damping constant, respectively.

$$M\Delta\dot{\omega} = -D\Delta\omega + P_m + U_m^2 Y_m \sin(\theta_m) + U_m U Y_m \sin(\delta - \delta_m - \theta_m) \tag{3}$$

where P_m, U_m, U, δ, Y_m and θ_m are mechanical power of generator, generator voltage, load voltage, load angle, Line 1 admittance and its angle, respectively.

In this study, the load bus feeds a constant PQ load and an induction motor in parallel. The load model is expressed by Eqs. (4) and (5).

$$P = P_0 + P_1 + k_{pw}\dot{\delta} + k_{pu}\left(U + T\dot{U}\right) \tag{4}$$

$$Q = Q_0 + Q_1 + k_{qw}\dot{\delta} + k_{qu}U + k_{qu2}U^2 \tag{5}$$

where Q_1 and P_1 denote the reactive and active power of the constant load, Q_0 and P_0 denote the constant part of the reactive and active power of the induction motor, and T is time constant. k_{pw}, k_{pu}, k_{qw}, k_{qu} and k_{qu2} are active load constant due to frequency deviation, active load constant due to voltage deviation, reactive load constant due to frequency deviation, reactive load constant due to voltage deviation, and reactive load constant due to voltage square deviation, respectively [29].

2.2. SVC

SVC is a static var absorber or generator, the output of which is adjusted to exchange inductive or capacitive current to control or maintain specific parameters of power systems (usually bus voltage) [30]. The SVC operation is based on adjustable susceptance. As in general, the purpose of using SVC is reactive power and voltage drop compensation, typically the SVC susceptance is determined according to the voltage error. The conventional control system of SVC is represented in Fig. 3 [31]. This controller generates the reference susceptance for the SVC operation that should be achieved by proper switching of the SVC.

From Fig. 3, Eq. (6) can be written.

$$\frac{dB}{dt} = \frac{k}{T_S}(U_{ref} - U) - \frac{B_{svc}}{T_S} \tag{6}$$

in which

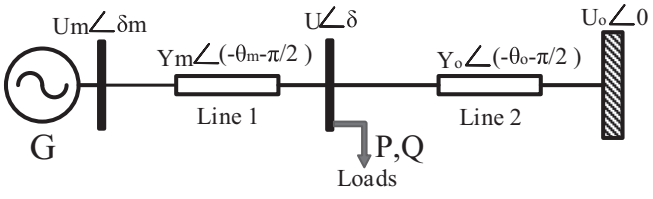

Fig. 2. A simple schematic of a SMIB system.

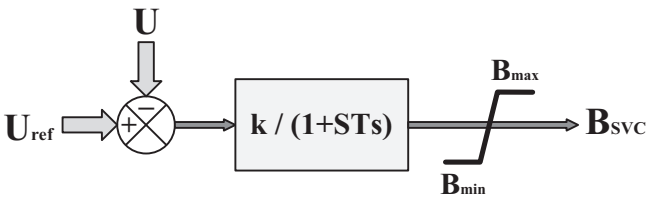

Fig. 3. The conventional control system of the SVC.

$$B_{svc} = B_C - B_L \tag{7}$$

where k, U_{ref}, T_S, B_{SVC}, B_C and B_L are the SVC gain, the reference voltage, the time constant of SVC, the SVC susceptance and its capacitive and inductive susceptance, respectively. The SVC used in this paper consists of three TSC units and one TCR unit. B_{SVC} determines the firing angle (α) of the TCR and the status (off/on) of the three TSC branches. α that is a function of the TCR susceptance (B_L) can be implemented using a look-up table formed according to Eq. (8):

$$B_L = \frac{2(\pi - \alpha) + \sin(2\alpha)}{\pi} \tag{8}$$

in which B_L is a per-unit value according to the rated reactive power of the TCR. Due to the use of the look-up-table to obtain α, B_{SVC} should be limited in the range defined for the input of the look-up-table ($B_{min} < B_{SVC} < B_{max}$) as represented in Fig. 3.

The equivalent reactive power flow of the SVC to the system can be calculated from Eq. (9).

$$Q_{svc} = B_{svc}U^2 \tag{9}$$

Considering the SVC effect on the reactive power flow of the system, Eq. (5) can be rewritten as Eq. (10). Also, by multiplying k_{qw} in Eq. (4), substituting Eq. (10) in Eq. (4), and using some mathematical simplifications, Eq. (11) will be obtained. So, by considering the effect of the SVC, the system model equations can be expressed as follow:

$$k_{qw}\dot{\delta} = -k_{qu}U - k_{qu2}U^2 + Q - Q_0 - Q_1 + Q_{svc} \tag{10}$$

$$Tk_{qw}k_{pu}\dot{U} = k_{pw}k_{qu2}U^2 + U(k_{pw}k_{qu} - k_{qw}k_{pu}) - k_{pw}(Q - Q_0 - Q_1 + Q_{svc}) + k_{qw}(P - P_0 - P_1) \tag{11}$$

2.3. DFIG

DFIG is among the generator types that are commonly used in wind farms. DFIG has several advantages such as low size, low converter power rating that leads to less converter cost, capability to control reactive and active power independently, and ability to work with variable wind speeds [12,32]. In DFIGs, the rotor is connected to the grid through two back-to-back converters and the stator is connected to the grid without any additional devices [33]. The ability of operation with variable wind speed is made possible by decoupling the electrical frequency from the mechanical frequency using the converters. Considering that the rated power of the converters is much smaller than the machine, the converters have low power losses and implementation cost [34]. In addition, it causes the turbine speed to be finite to a certain but sufficient range [35].

Using the transformation of the abc reference frame to the dq reference frame, a simple DFIG model can be obtained with the following voltage equations. The transformation matrix to convert the abc reference frame to the dq reference frame (the Park's transformation) is given in Appendix 1. The subscripts 'r' and 's' respectively denote the rotor and the stator parameters.

$$\bar{U}_s = r_s\bar{i}_s + \frac{d\bar{\varphi}_s}{dt} + j\omega_{dq}\bar{\varphi}_s \tag{12}$$

$$\bar{U}_r = r_r\bar{i}_r + \frac{d\bar{\varphi}_r}{dt} + j(\omega_{dq} - \omega_e)\bar{\varphi}_r \tag{13}$$

where r is the resistance, ω_{dq} is the rotating speed of the dq frame, and ω_e is the rotor electrical angular speed. The magnetic flux vector φ can be achieved from Eqs. (14) and (15):

$$\bar{\varphi}_s = \bar{i}_s L_s + \bar{i}_r L_m \tag{14}$$

$$\bar{\varphi}_r = \bar{i}_s L_m + \bar{i}_r L_r \tag{15}$$

where L is the inductance and L_m indicates the magnetizing inductance. Considering the previous equations, the following voltage equations can be achieved:

$$\bar{U}_s = \frac{d\bar{\varphi}_s}{dt} + \left(\frac{r_r}{L_r} + j\omega_{dq}\right)\bar{\varphi}_s - \frac{L_m r_s}{L_r L_s}\bar{\varphi}_r \tag{16}$$

$$\bar{U}_r = \frac{d\bar{\varphi}_r}{dt} + \left(\frac{r_r}{L_r} + j(\omega_{dq} - \omega_e)\right)\bar{\varphi}_s - \frac{L_m r_r}{L_r L_s}\bar{\varphi}_s \tag{17}$$

Fig. 4 presents the equivalent circuit of the DFIG dynamic model achieved from the aforementioned equations [36].

In this paper, a DFIG-based wind farm is considered as the single generator in the SMIB system. Fig. 5 presents the overall schematic of the test system. In order to enhance the SVC performance in voltage stabilization, an auxiliary control signal is added to the SVC controller given in Fig. 3. This auxiliary control signal is generated using a fuzzy inference system (FIS). This signal modifies the input of the transfer function that generates the reference susceptance and by adding a supplementary voltage control to the controller leads to the enhancing the control system accuracy in generating the reference susceptance of the SVC. Therefore, the SVC with the proposed supplementary FC will have more accuracy in voltage regulation in the steady state and will show better transient under the fault situation. The details regarding the FC design is explained in Section 3.

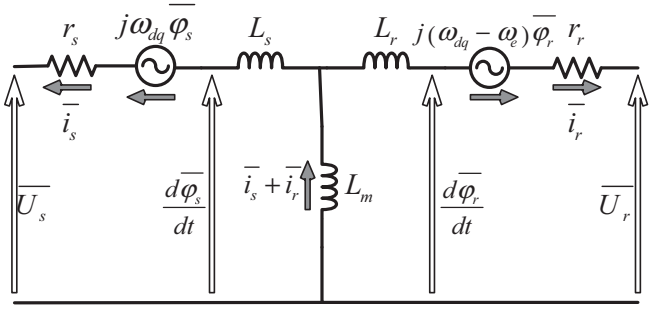

Fig. 4. The equivalent circuit of the DFIG dynamic model.

3. Proposed FC for SVC

The fuzzy logic is a mathematical tool to make decisions despite the uncertainties. Unlike the two-valued logic in which a proposition is either false (0) or true (1), in fuzzy logic, a proposition can be somewhat true. Input data of a fuzzy system can be linguistic variables, like many, few, high, low, medium, etc. [37]. A FIS consists of four parts [38]:

1) Fuzzifier part: In this part, each input is transformed to a fuzzy variable according to the defined membership functions.
2) Knowledgebase part: This part consists of fuzzy rules and information of the system, which are used by the inference engine.
3) Fuzzy inference part: This part is the decision unit and owing to its inputs from fuzzifier and the knowledge base, performs fuzzy inference.
4) Defuzzifier part: In this part, the fuzzy inference engine output is transformed into a crisp signal usable by the control system. Center of area (COA), center of gravity (COG), center of maximum (COM), center of sums (COS), and mean of maximum (MOM) methods are some of the defuzzification techniques. The defuzzification method used in this paper is COG which is one of the most prevalent ones among the mentioned methods and because of continuity and, often, smoothness of the changes of defuzzified values has been widely used in FCs.

The fuzzy logic (FL) has several advantages and some disadvantages. Some advantages of FL are: simple and comprehensible structure; ability to model the nonlinear functions with any degree of complexity; capability to be merged with conventional classic control methods for increasing their efficiency; workability in situ-

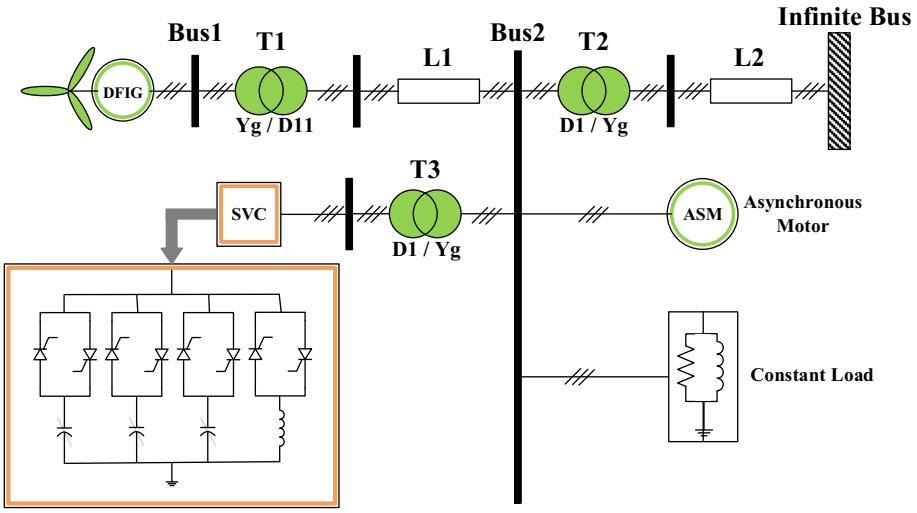

Fig. 5. The overall schematic of the test system.

ations where the data is inaccurate, so it can be used in noisy environments, in addition, it leads to the reducing the cost of sensors; ability to provide response with low overshoot and oscillation; finally, capability to represent the uncertainties of human knowledge with linguistic variables. Some of the disadvantages are: there is not any standard procedure for transformation the human knowledge to fuzzy rules; being unable to be generalized, i.e., only responds based on the rule base and is dependent on the existence of an expert to define the fuzzy rules [39–42].

In the following, the design procedure of the proposed FC is explained. There are three main steps in designing an FC;

First, the inputs and outputs of the FC should be determined according to its application.

Since in this work, the FC is employed to improve the SVC performance in adjusting the voltage and enhancing the voltage stability of the system, so the voltage (per-unit) and its time derivative are considered as the FC inputs, and its output is an auxiliary signal (U_f) that modifies the reference susceptance of the SVC, which determines the firing angle. It is worth mentioning that the time derivative of the voltage is considered as one of the fuzzy inputs to enable the FC to make proper decisions based on not only the current state of the voltage, but also its future state. In general, this ability is one of the factors that make FCs superior to conventional controllers.

Second, the most proper membership functions should be defined according to the specifications of each type of membership functions and the FC designer's knowledge regarding the system behavior.

Various types of membership functions can be used in a FIS, and each type has its own specifications. For example, the triangular membership function provides a linear relation between the variations of the input and the output signal. This type of membership functions are useful in the systems that the control signal should linearly respond to the changes of the controlled parameter to make the controller operate properly. In the trapezoidal membership function, the control signal will remain unchanged for the changes of the input signal in a certain range. This type will be useful for the systems that a range of the controlled parameter value is acceptable and its variations in the mentioned range do not need to make any change in the control signal. In the Gaussian membership function, a small change in the controlled parameter leads to a small variation in the control signal and the controller will strongly respond to the high variations of the controlled parameter. According to the system characteristics and the simulations performed, this type of membership functions is employed in the proposed FC.

In addition to the selection of proper membership functions, defining proper ranges for fuzzy variables is also so important in designing an FC. Usually, defining symmetric ranges for the fuzzy variables makes defining the fuzzy rules more straightforward and leads to better results. In this work, the range of the first FC input (voltage) is considered between 0 and 2, because it is a per-unit value, so this symmetric range can cover properly all changes in this controlled parameter. The range of the second FC input (voltage deviation) is chosen between −1 to 1. This range has been obtained according to the range of possible variations achieved by the simulations. The range of FC output is considered between −1 and 1. Because in this work, the minimum and the maximum value of the reference susceptance of the SVC are considered as 0 and 1 (Appendix 2), so variations of U_f should be in the range of [−1,1] and its value out of this range will be effectless in the controller performance as it will be saturated.

The membership functions considered for the two inputs and the output of the proposed FC are given in Fig. 6. The linguistic variables assigned for each variable are "Positive Big" (PB), "Positive Medium" (PM), "Positive Small" (PS), "Zero" (Z), "Negative Small" (NS), "Negative Medium" (NM) and "Negative Big" (NB).

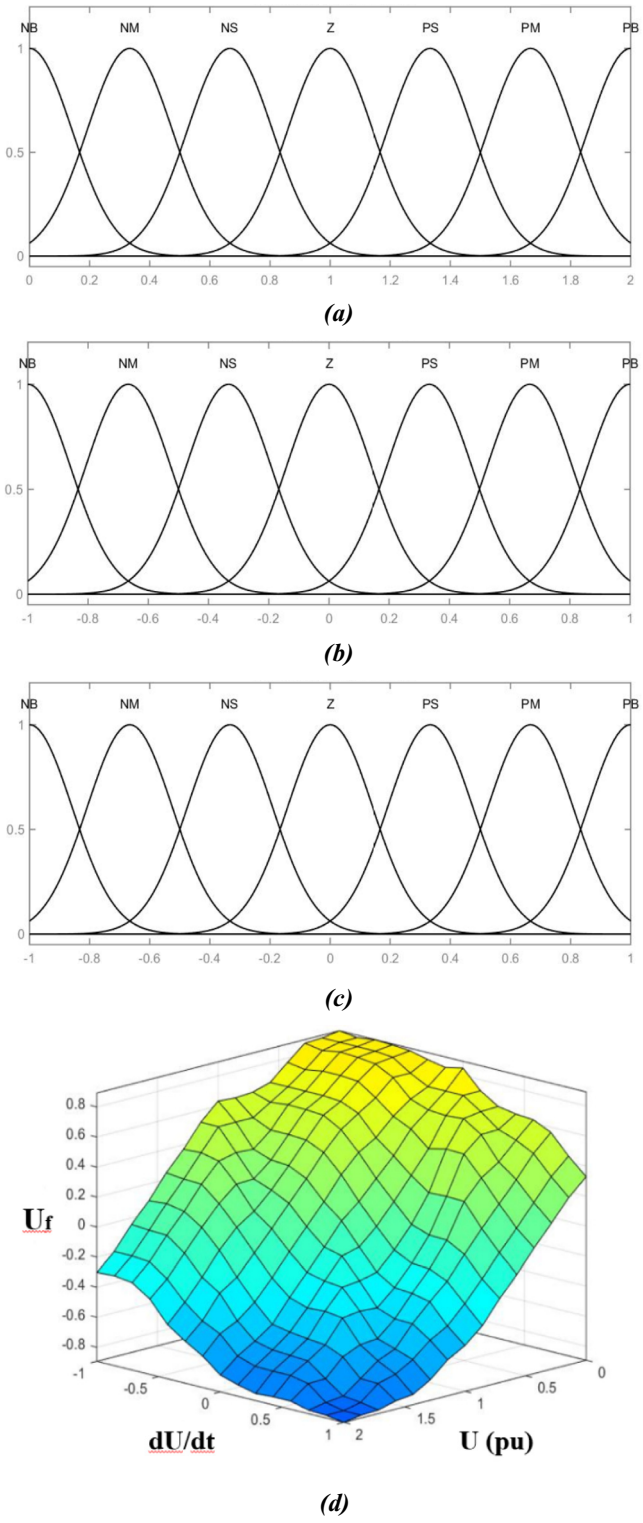

Fig. 6. Membership functions and rules surface view of the FC; (a) membership functions of load bus voltage (p.u.) as FC input, (b) membership functions of time derivative of load bus voltage (p.u.) as FC input, (c) membership functions of auxiliary signal Uf as FC output, (d) the surface view of the FC rules.

Third, the fuzzy rule base should be defined according to the FC designer's knowledge with respect to the system behavior to realize the control objectives.

Table 2
The rule base of the proposed FC.

U (pu) dU/dt	NB	NM	NS	Z	PS	PM	PB
NB	PB	PB	PM	PM	PS	Z	NS
NM	PB	PB	PM	PS	PS	Z	NS
NS	PB	PB	PM	PS	Z	NS	NM
Z	PB	PM	PS	Z	NS	NM	NB
PS	PM	PM	Z	NS	NS	NM	NB
PM	PM	PS	Z	NS	NM	NB	NB
PB	PS	Z	NS	NM	NB	NB	NB

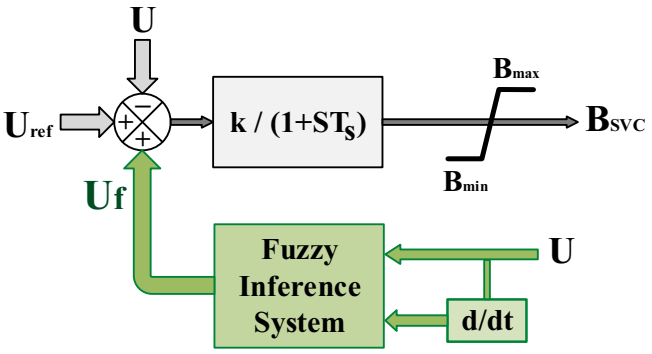

Fig. 7. The schematic of the proposed control system.

In this work, the fuzzy rules should be determined based on the SVC operational principles; we know that an increment in the reference susceptance of the SVC results in the injecting more reactive power and increasing the voltage consequently, so this is the basis of the definition of the fuzzy rules. For instance, if the bus voltage is NB (high voltage shortage) and its derivative is NB (the voltage is quickly decreasing), then the reference susceptance of the SVC (the control signal) should be strongly increased to compensate this defect, so the value of the supplementary control signal U_f should be chosen as PB. The rest of the fuzzy rules have been also determined with similar inferences. All fuzzy rules are listed in Table 2 and the surface plot of them is indicated in Fig. 6d. The schematic of the proposed controller is also presented in Fig. 7.

4. Simulation results

In this section, the performance of the suggested control technique is investigated and its effectiveness is verified by system simulations in MATLAB/Simulink. The system parameters are given in Appendix 2, the wind speed profile is shown in Fig. 8, and the Simulink block diagram of the system is presented in Fig. 9. To properly study the SVC performance, different reactive power demands are considered in the test system; simulations have been done for three different values of the constant load, which are listed in Table 3. Also, to investigate the system performance under the fault situation, a temporary three-line to ground fault for 100 ms is applied to the load bus at 6 S.

The per-unit voltage of Bus 2 using the conventional SVC (CSVC) and the proposed fuzzy-based SVC (FSVC) with load 1, 2 and 3 is shown in Fig. 10. According to this figure, the use of the proposed FC for the SVC has increased the performance accuracy of the controller that results in enhancing the steady state voltage of the load bus and decreasing the maximum voltage drop after the fault occurrence. To better show the performance of the SVC controller, the susceptance variations of the CSVC and the FSVC with load 1, 2 and 3 are presented in Fig. 11. According to Figs. 10 and 11, the SVC controller compensates the voltage shortage or abundance from 1 pu by increasing or decreasing the reference B_{SVC}. Due to the

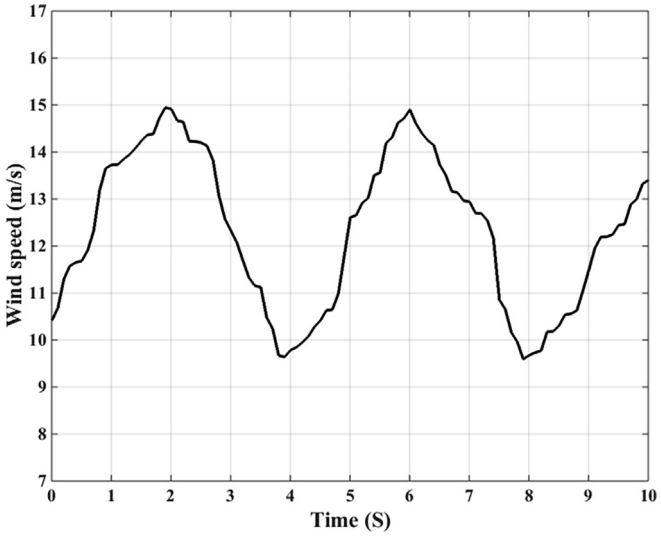

Fig. 8. The wind speed profile.

increasing the controller accuracy using the proposed FC, the system response with FSVC is more desirable than CSVC as the SVC controller by using the FC can determine more precisely the required amount of reactive power that should be injected to or absorbed from the system to make the bus voltage as much closer as possible to its nominal value.

Fig. 12 shows the per-unit voltage of Bus 1 using CSVC and FSVC with load 1, 2 and 3. According to this figure, the voltage drop at Bus 1 using FSVC is less than CSVC, which leads to the enhancing the LVRT capability of the wind farm, and consequently, improving the system stability and resiliency. This achievement is among the most outstanding findings in this research as by proposing a relatively simple fuzzy-based supplementary control loop added to the control system of the SVC employed for stability improvement, we have also enhanced the LVRT capability of the wind farm, while the common existing techniques for this purpose are usually more complicated and expensive.

The steady state voltage error of Bus 2, with different load values using CSVC and FSVC is illustrated in Fig. 13a. As it is clear in this figure, the steady state voltage error using FSVC is significantly less than CSVC in all cases. The maximum voltage drop from 1p.u. after the fault occurrence, related to Bus 1 and Bus 2, with different load values using CSVC and FSVC is presented in Fig. 13b. According to this figure, the maximum voltage drop using FSVC is less than CSVC. Also, for more clarity, the numerical data with respect to Fig. 13 is given in Table 4. Notice that the voltage of Bus 1 with load 1 using CSVC is unable to satisfy the GCR while FSVC has been able to maintain it in the acceptable area specified by the grid code. According to Table 4, in the system simulation with load 1, 2, and 3, the proposed FC has been able to decrease the steady state voltage error at Bus 2 by 75.93, 86.25, and 61.14%, and the maximum voltage drop after the fault occurrence at Bus 1 by 31.19, 23.92, and

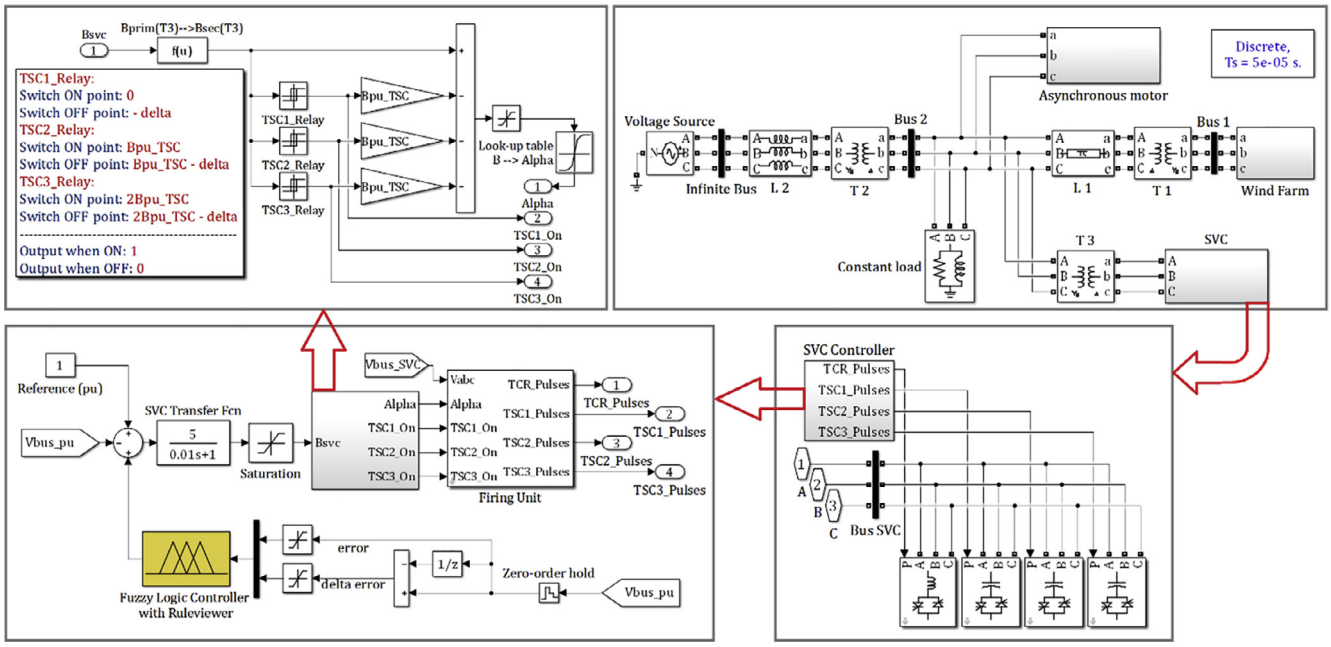

Fig. 9. The Simulink block diagram of the system.

Table 3
The different values of the constant load in the simulated system.

	P (pu)	Q (pu)
Load 1	0.9	1.5
Load 2	0.9	3.0
Load 3	0.9	4.0

20.36%, respectively. So, in this test system considering the case studies, on average, the proposed FC has decreased the steady state voltage error and the maximum voltage drop under the fault situation by 74.44 and 25.16%, respectively.

The system frequency measured at Bus 2 while using CSVC and FSVC with load 1, 2 and 3 is shown in Fig. 14. In the results obtained, the maximum frequency variations relative to the nominal frequency, which is calculated by (18), for the three cases is as follow:

Load 1 with CSVC: 0.7167%, with FSVC: 0.5667%
Load 2 with CSVC: 0.6250%, with FSVC: 0.5250%
Load 3 with CSVC: 0.6417%, with FSVC: 0.5830%

$$FV(\%) = \frac{|\Delta f|_{max}}{f_{nominal}} \times 100 \qquad (18)$$

As it is clear in these results, another advantage of using the proposed fuzzy control technique in this system is that it provides less frequency variations under the system disturbances. In the power system operation, this matter is of utmost importance as it can dramatically affect the performance of the loads. For instance, in [43], the impact of frequency variations on the performance of AC induction motors is investigated and according to the obtained results, it can have significant negative effects on the motor operating costs, performance characteristics and life expectancy.

According to the simulation results, because of using the proposed FC for the SVC, the stability and robustness of the system have been improved and the LVRT capability of the wind farm has been enhanced. By using FSVC, the system is capable to maintain the load bus voltage in the acceptable area (1 ± 0.05 p.u.) and satisfy the GCRs in a larger range of load variations in comparison to the case that CSVC has been employed.

The more accurate voltage stabilization using the FSVC and its better transient response have also suitable effects on the performance of the DFIG-based wind turbine. The DFIG rotor speed (per-unit) and the blade pitch angle of the wind turbine while using CSVC and FSVC with different load values are presented in Figs. 15 and 16, respectively. As it is visible in these figures, due to the less voltage drop under the fault situation by using the proposed fuzzy controller, the variations imposed to the DFIG-based wind turbine operation are less than the case that the conventional technique is used to control the SVC.

5. Further discussions and future works

In this section, first, we discuss the reasons that make the control systems designed based on fuzzy logic superior to the traditional ones that are designed based on a simplified model of the system and are implemented using transfer functions, and then we will provide some suggestions for possible future works.

As we saw in the simulation results, the effectiveness and the accuracy of the FSVC is better than CSVC. This is originated from the way that these controllers are designed. In general, since there is more freedom in designing a fuzzy controller, we can design it more accurately by considering the different conditions of the system operation. In traditional controllers that are modeled using one or more transfer functions, the coefficients of the transfer functions are usually tuned according to the stable operating point of the system. While, in designing a fuzzy controller, we can define distinct rules for different operating points of the system. For instance, in a traditional controller, we might need to set a high value for the proportional gain of the transfer function to achieve a suitable response under a sort of system disturbances. However, we cannot do that due to the stability considerations of the system as such a high gain will not be workable at the stable operating point. While we do not have such restrictions in designing a fuzzy controller. In other words, a fuzzy controller by having a well-defined rule base can perform like a traditional controller that is

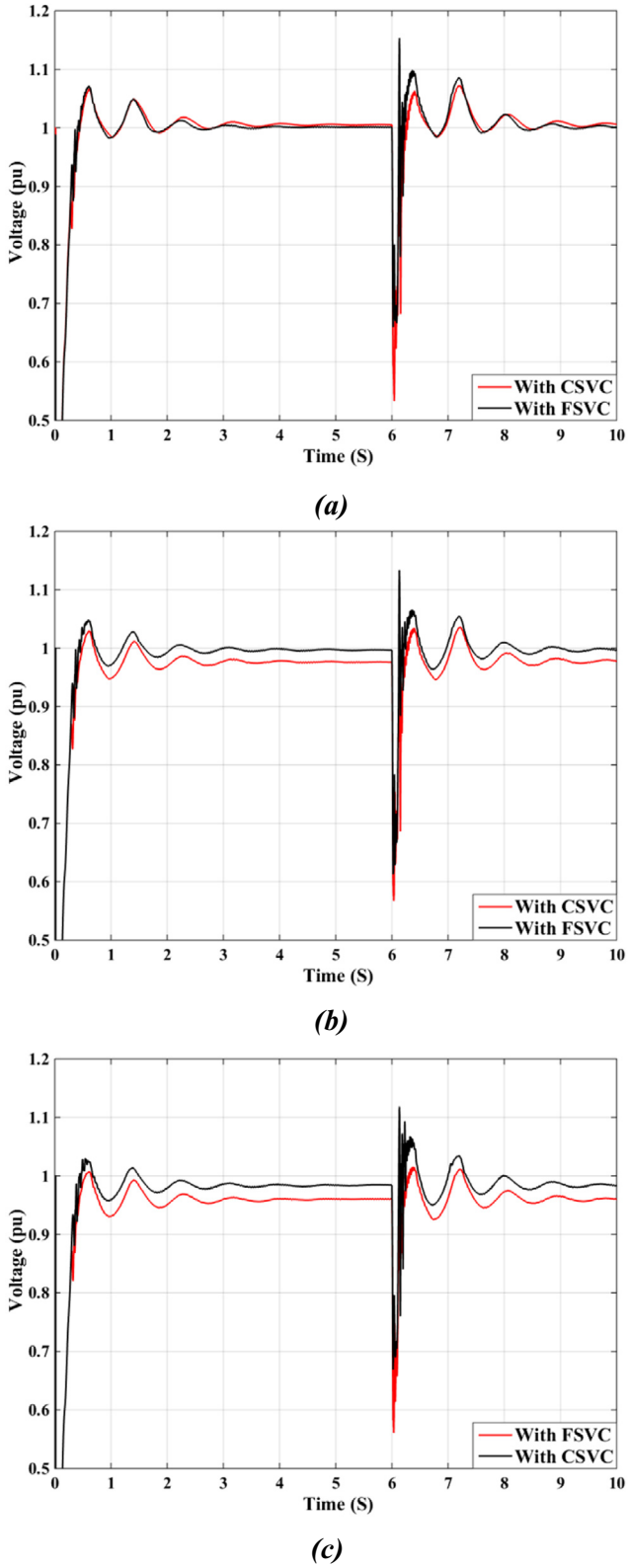

Fig. 10. Voltage of bus 2 using CSVC and FSVC; (a) with load 1, (b) with load 2, (c) with load 3.

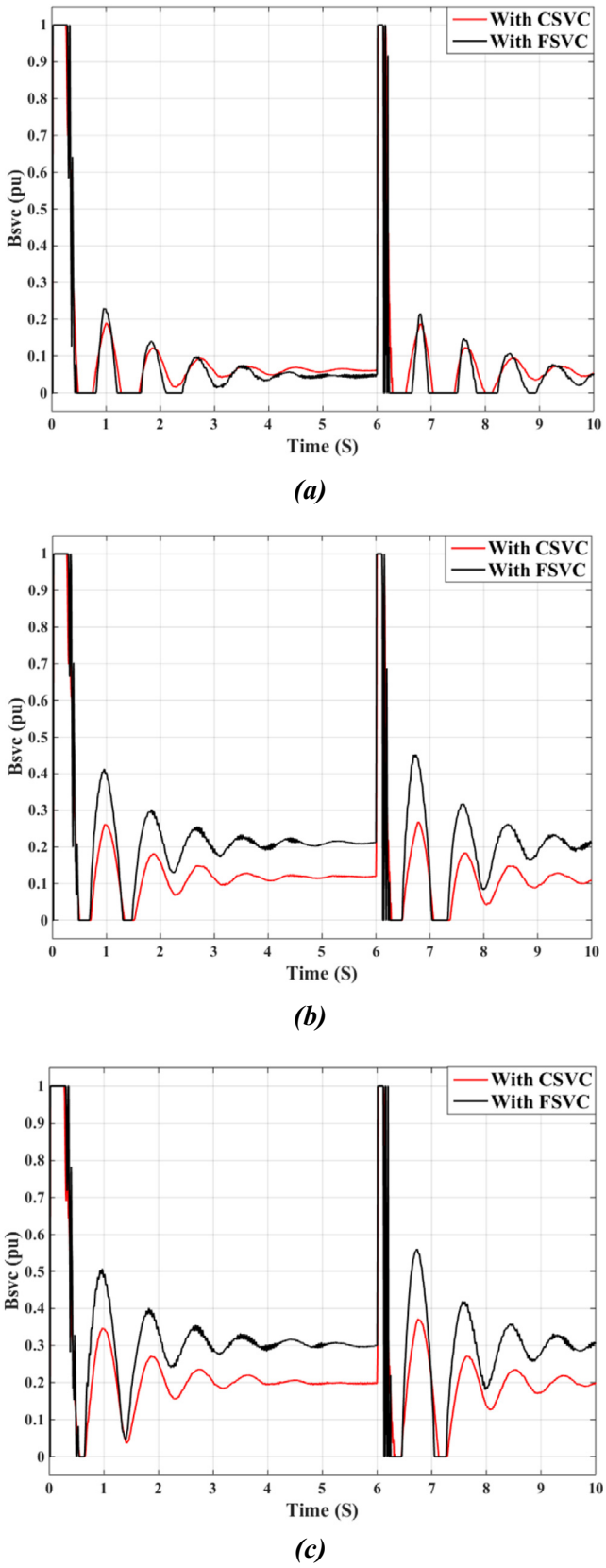

Fig. 11. The reference susceptance of CSVC and FSVC; (a) with load 1, (b) with load 2, (c) with load 3.

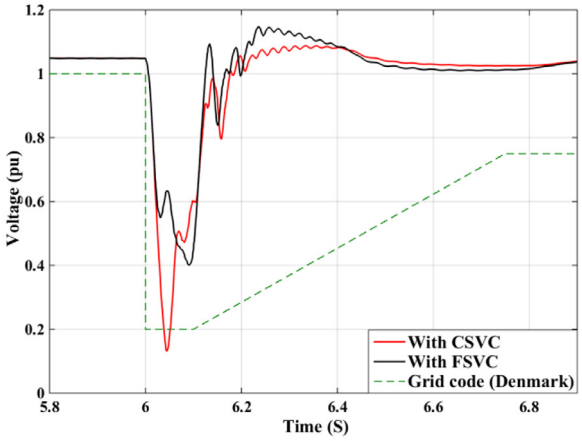

(a)

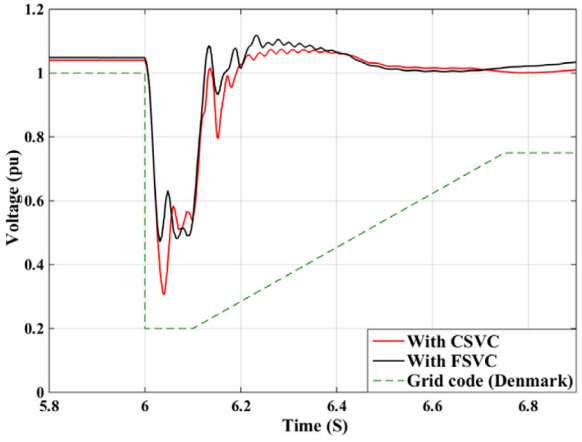

(b)

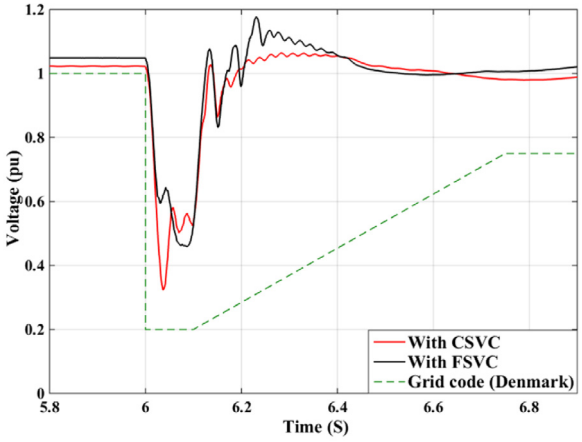

(c)

Fig. 12. Voltage of bus 1 using CSVC and FSVC; (a) with load 1, (b) with load 2, (c) with load 3.

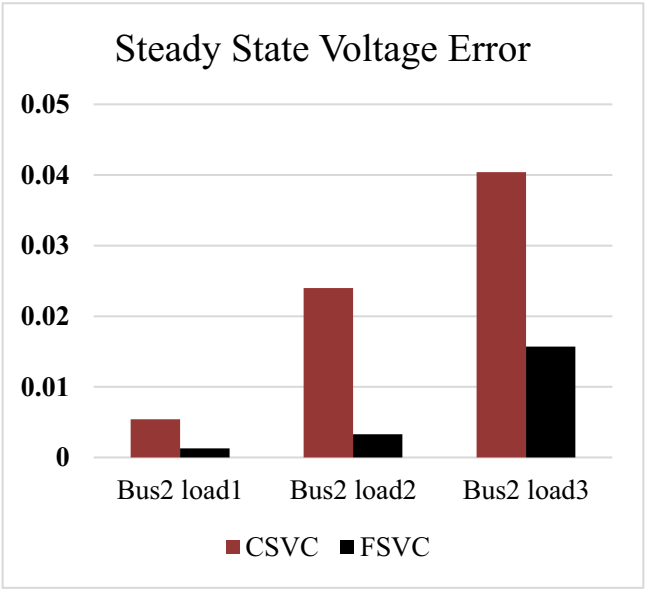

(a)

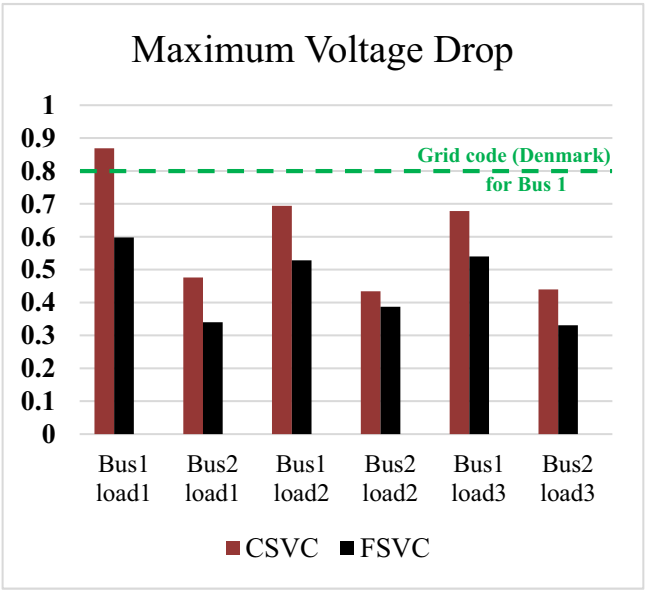

(b)

Fig. 13. The steady state voltage error (a) and the maximum voltage drop after fault occurrence (b) using CSVC and FSVC.

able to dynamically change its coefficients according to the system requirements. Therefore, fuzzy controllers have more flexibility and accuracy in their operation and respond better in the transient state.

Table 4
Comparison between the performance of CSVC and FSVC.

SCV type	Normal operation			After fault occurrence					
	Steady state voltage error			Maximum Voltage Drop					
	Bus 2			Bus 1			Bus 2		
	Load 1	Load 2	Load 3	Load 1	Load 2	Load 3	Load 1	Load 2	Load 3
CSVC	0.0054	0.0240	0.0404	0.869	0.694	0.678	0.476	0.434	0.440
FSCV	0.0013	0.0033	0.0157	0.598	0.528	0.540	0.340	0.387	0.331

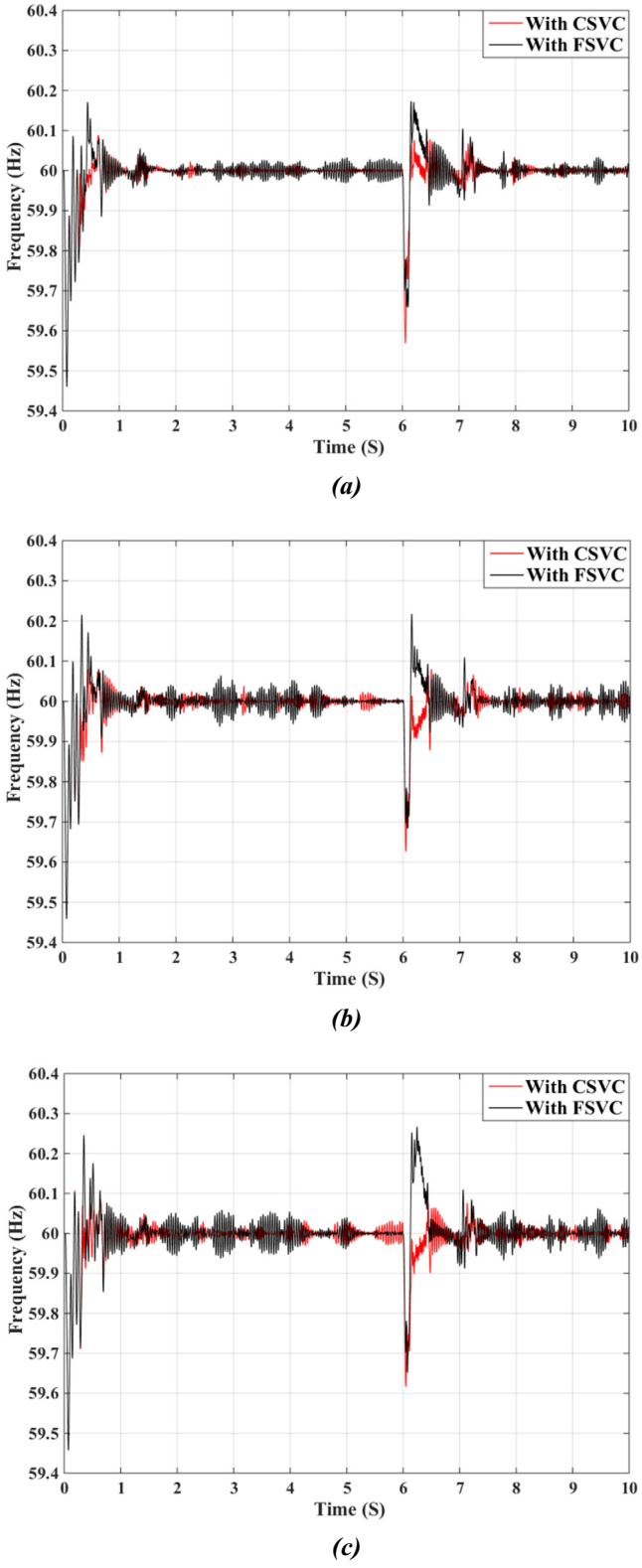

Fig. 14. System frequency measured at bus 2 while using CSVC and FSVC; (a) with load 1, (b) with load 2, (c) with load 3.

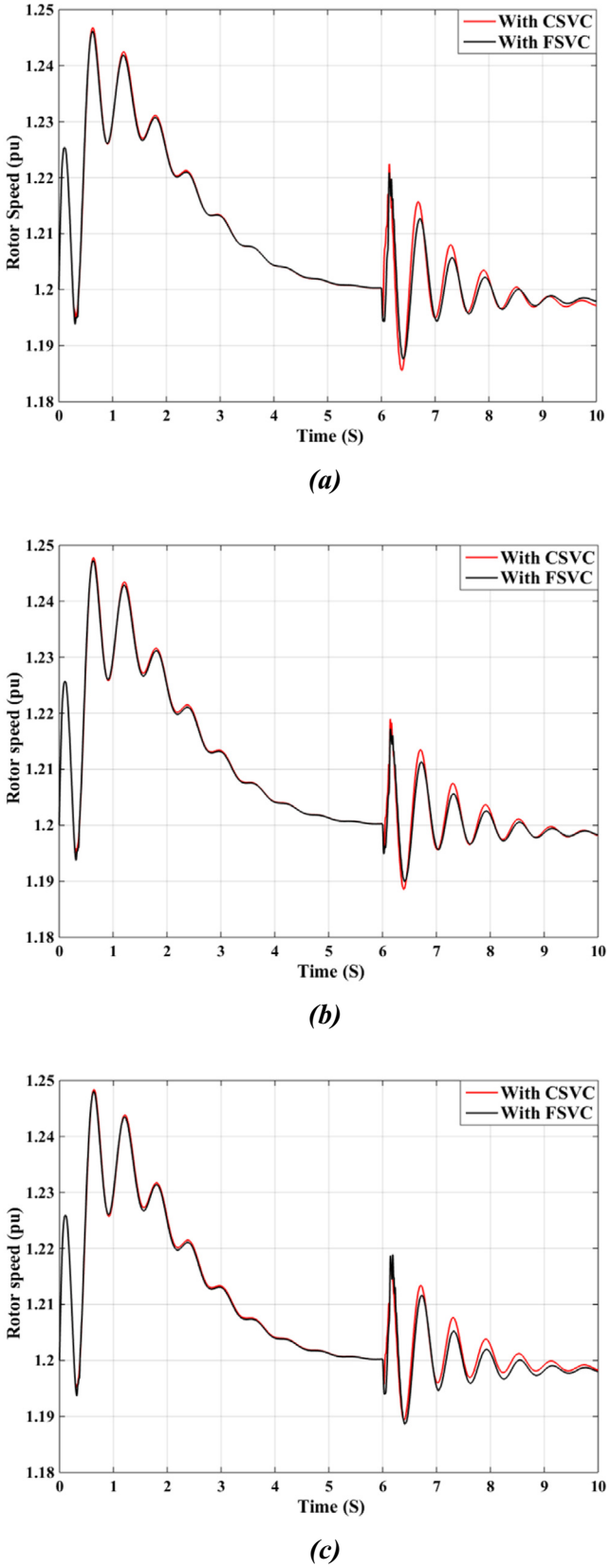

Fig. 15. The DFIG rotor speed using CSVC and FSVC; (a) with load 1, (b) with load 2, (c) with load 3.

Another important point regarding the fuzzy controllers that makes them superior to traditional controllers is that by using them, we can easily model non-linear functions with any degree of complexity. Most of the traditional controllers are designed using linear functions while having many simplifications in the system model, one the reasons of which is that tuning non-linear functions is too hard and even impossible especially in complex systems. So, in such situations by utilizing the simple concept of

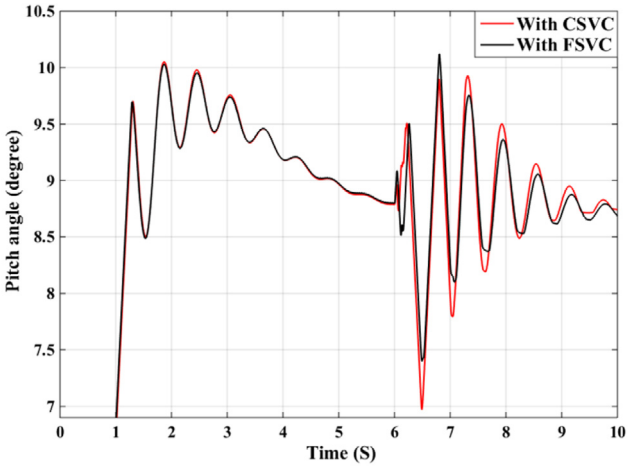

(a)

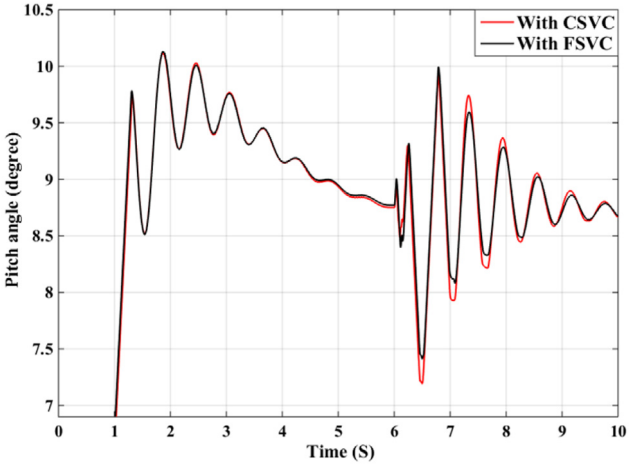

(b)

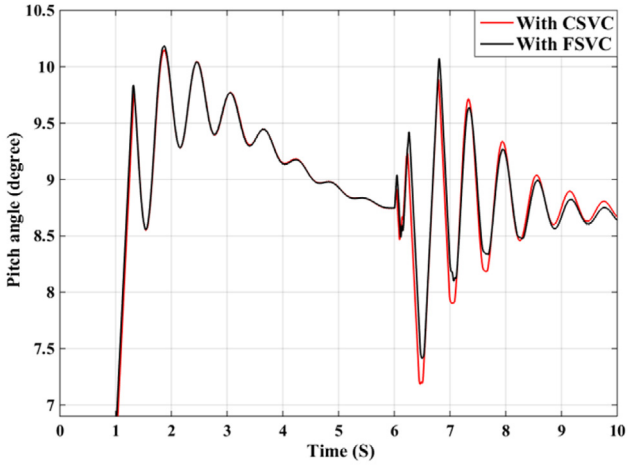

(c)

Fig. 16. The blade pitch angle using CSVC and FSVC; (a) with load 1, (b) with load 2, (c) with load 3.

fuzzy logic and by having enough knowledge about the system, we can easily design a controller that performs like a highly complex non-linear controller to realize our control objectives.

Suggestions for future research works: a) Employing other intelligent control techniques with more adaptability such as ANFIS to generate the auxiliary control signal more accurately, b) Replacing the SVC controller by a fully fuzzy controller (omitting the transfer function from the SVC controller) to further improve the SVC performance, and c) Employing the proposed fuzzy-based SVC for other applications such as harmonic compensation by modifying the FIS.

6. Conclusion

This paper investigated the SVC impact on the stability improvement and LVRT capability enhancement in a SMIB system with a DFIG-based wind farm. The SVC performance in this test system is enhanced by integrating a proposed FIS to the SVC controller. In the proposed method, an auxiliary control signal generated by the proposed FC is added to the conventional control system of the SVC that leads to the decreasing the steady state voltage error and the maximum voltage drop after the fault occurrence. Because of the less voltage drop under the fault situation using the proposed FC for the SVC, the LVRT capability of the wind farm is improved and the system capability to meet the GCRs is enhanced. The effectiveness of the suggested control technique is confirmed and its effect on the behavior of the DFIG-based wind turbine is investigated using system simulations in MATLAB/Simulink.

Conflict of interest

There is no conflict of interest.

Appendix 1. The Park's transformation

$$x_{dq0} = Kx_{abc} = \sqrt{\frac{2}{3}}\begin{bmatrix} \cos(\theta) & \cos\left(\theta-\frac{2\pi}{3}\right) & \cos\left(\theta+\frac{2\pi}{3}\right) \\ -\sin(\theta) & -\sin\left(\theta-\frac{2\pi}{3}\right) & -\sin\left(\theta+\frac{2\pi}{3}\right) \\ \frac{\sqrt{2}}{2} & \frac{\sqrt{2}}{2} & \frac{\sqrt{2}}{2} \end{bmatrix} . \begin{bmatrix} x_a \\ x_b \\ x_c \end{bmatrix}$$

Appendix 2. Test system parameters

System base parameters	
Base power (MVA)	10
Base frequency (Hz)	60
Base angular frequency (rad/s)	120π
DFIG-based wind farm	
Number of wind turbines	6
Generators parameters	
Nominal power (MVA)	1.667
Nominal stator voltage (Vrms)	575
Nominal rotor voltage (Vrms)	1975
Stator resistance (pu)	0.023
Stator inductance (pu)	0.18
rotor resistance (pu)	0.016
rotor inductance (pu)	0.16
Magnetizing inductance (pu)	2.9
Inertia constant (S)	0.685
Friction factor (pu)	0.01

(*continued on next page*)

Turbines parameters	
Nominal mechanical output power (MW)	1.5
Wind speed at nominal speed and at Cp max (m/s)	11
Maximum pitch angle (deg)	27
Maximum rate of change of pitch angle (deg/s)	10
T1	
Winding primary connection	D 11
Winding secondary connection	Yg
Nominal power (MVA)	10.5
Primary phase to phase voltage (kVrms)	25
Primary resistance (pu)	0.0008
Primary inductance (pu)	0.025
Secondary phase to phase voltage (kVrms)	0.575
Secondary resistance (pu)	0.0008
Secondary inductance (pu)	0.025
T2	
Winding primary connection	Yg
Winding secondary connection	D 1
Nominal power (MVA)	47
Primary phase to phase voltage (kVrms)	120
Primary resistance (pu)	0.0027
Primary inductance (pu)	0.08
Secondary phase to phase voltage (kVrms)	25
Secondary resistance (pu)	0.0027
Secondary inductance (pu)	0.08
T3	
Winding primary connection	Yg
Winding secondary connection	D 1
Nominal power (MVA)	50
Primary phase to phase voltage (kVrms)	25
Primary resistance (pu)	0.0025
Primary inductance (pu)	0.105
Secondary phase to phase voltage (kVrms)	16
Secondary resistance (pu)	0.0025
Secondary inductance (pu)	0.045
L1	
Positive sequence resistance (Ω)	3.459
Positive sequence inductance (H)	0.0315
Positive sequence capacitance (μF)	0.3399
Zero sequence resistance (Ω)	12.39
Zero sequence inductance (H)	0.0996
Zero sequence capacitance (μF)	0.1503
L2	
Positive sequence resistance (Ω)	0.576
Positive sequence inductance (H)	0.0153
Positive sequence capacitance (μF)	0
Zero sequence resistance (Ω)	17.28
Zero sequence inductance (H)	0.0458
Zero sequence capacitance (μF)	0
Asynchronous motor (ASM)	
Nominal power (MVA)	16.785
Nominal stator voltage (kVrms)	25
Stator resistance (Ω)	0.029
Stator inductance (H)	0.599
rotor resistance (Ω)	0.022
rotor inductance (H)	0.599
Mutual inductance (H)	0.034
Inertia (kg.m^2)	63.87
Rotor type	Squirrel-cage
SVC	
SVC gain k	5
SVC time constant Ts	0.01
Bmin	0
Bmax	1

References

[1] H. Rezaie, M.H. Kazemi-Rahbar, B. Vahidi, H. Rastegar, Solution of combined economic and emission dispatch problem using a novel chaotic improved harmony search algorithm, J. Comput. Des. Eng. (2018), https://doi.org/10.1016/j.jcde.2018.08.001.

[2] S.S. Reddy, J.A. Momoh, Realistic and transparent optimum scheduling strategy for hybrid power system, IEEE Trans. Smart Grid 6 (6) (2015) 3114–3125.

[3] S.S. Reddy, Optimal scheduling of thermal-wind-solar power system with storage, Renewable Energy 101 (2017) 1357–1368.

[4] S.S. Reddy, Optimal scheduling of wind-thermal power system using clustered adaptive teaching learning based optimization, Electr. Eng. 99 (2) (2017) 535–550.

[5] J.A. Momoh, S.S. Reddy, Y. Baxi, Stochastic voltage/Var control with load variation, in: PES General Meeting| Conference & Exposition, IEEE, 2014, pp. 1–5.

[6] B. Lu, M. Shahidehpour, Short-term scheduling of battery in a grid-connected PV/battery system, IEEE Trans. Power Syst. 20 (2) (2005) 1053–1061.

[7] J.F. Conroy, R. Watson, Low-voltage ride-through of a full converter wind turbine with permanent magnet generator, IET Renewable Power Gener. 1 (3) (2007) 182–189.

[8] M.J. Hossain, H.R. Pota, R.A. Ramos, Improved low-voltage-ride-through capability of fixedspeed wind turbines using decentralised control of STATCOM with energy storage system, IET Gener. Transm. Distrib. 6 (8) (2012) 719–730.

[9] M. Liserre, R. Cardenas, M. Molinas, et al., Overview of multi-MW wind turbines and wind parks, IEEE Trans. Ind. Electron. 4 (58) (2011) 1081–1095.

[10] M.K. Döşoğlu, Nonlinear dynamic modeling for fault ride-through capability of DFIG-based wind farm, Nonlinear Dyn. 89 (4) (2017) 2683–2694.

[11] M. Tsili, S. Papathanassiou, A review of grid code technical requirements for wind farms, IET Renewable Power Gener. 3 (3) (2009) 308–332.

[12] H. Rezaie, S.M.M. Chashmi, M. Mirsalim, H. Rastegar, Enhancing LVRT capability and smoothing power fluctuations of a DFIG-based wind farm in a DC microgrid, Electr. Power Compon. Syst. 45 (10) (2017) 88–95.

[13] M.K. Döşoğlu, A.B. Arsoy, U. Güvenç, Application of STATCOM-supercapacitor for low-voltage ride-through capability in DFIG-based wind farm, Neural Comput. Appl. 28 (9) (2017) 2665–2674.

[14] M.K. Döşoğlu, A.B. Arsoy, Transient modeling and analysis of a DFIG based wind farm with supercapacitor energy storage, Int. J. Electr. Power Energy Syst. 78 (2016) 414–421.

[15] L. Qu, W. Qiao, Constant power control of DFIG wind turbines with supercapacitor energy storage, IEEE Trans. Ind. Appl. 47 (1) (2011) 359–367.

[16] N. Mendis, K.M. Muttaqi, S. Perera, Active power management of a super capacitor-battery hybrid energy storage system for standalone operation of DFIG based wind turbines, in: Industry Applications Society Annual Meeting (IAS), IEEE, 2012, pp. 1–8.

[17] K. Ghedamsi, D. Aouzellag, E.M. Berkouk, Control of wind generator associated to a flywheel energy storage system, Renewable Energy 33 (9) (2008) 2145–2156.

[18] B. Mahdad, K. Srairi, Adaptive differential search algorithm for optimal location of distributed generation in the presence of SVC for power loss reduction in distribution system, Eng. Sci. Technol. Int. J. 19 (3) (2016) 1266–1282.

[19] P. Kundur, N.J. Balu, M.G. Lauby, Power System Stability and Control, McGraw-hill, New York, 1994.

[20] T. Hiyama, M. Mishiro, H. Kihara, et al., Fuzzy logic switching of thyristor controlled braking resistor considering coordination with SVC, IEEE Trans. Power Delivery 10 (4) (1995) 2020–2026.

[21] B. Changaroon, S.C. Srivastava, D. Thukaram, et al., Neural network based power system damping controller for SVC, IET, IEE Proc. Gener. Transm. Distrib. 146 (4) (1999) 370–376.

[22] Q. Gu, A. Pandey, S.K. Starrett, Fuzzy logic control schemes for static VAR compensator to control system damping using global signal, Elsevier Electr. Power Syst. Res. 67 (2) (2003) 115–122.

[23] K.L. Lo, M.O. Sadegh, Systematic method for the design of a full-scale fuzzy PID controller for SVC to control power system stability, IET, IEE Proc. Gener. Transm. Distrib. 150 (3) (2003) 297–304.

[24] J. Wang, C. Fu, Y. Zhang, SVC control system based on instantaneous reactive power theory and fuzzy PID, IEEE Trans. Ind. Electron. 55 (4) (2008) 1658–1665.

[25] D.Z. Fang, Y. Xiaodong, T.S. Chung, et al., Adaptive fuzzy-logic SVC damping controller using strategy of oscillation energy descent, IEEE Trans. Power Syst. 19 (3) (2004) 1414–1421.
[26] L. Wang, D.N. Truong, Stability enhancement of a power system with a PMSG-based and a DFIG-based offshore wind farm using a SVC with an adaptive-network-based fuzzy inference system, IEEE Trans. Ind. Electron. 60 (7) (2013) 2799–2807.
[27] I.M. Ginarsa, A. Soeprijanto, M.H. Purnomo, Controlling chaos and voltage collapse using an ANFIS-based composite controller-static var compensator in power systems, Elsevier Int. J. Electr. Power Energy Syst. 46 (2013) 79–88.
[28] H. Huang, C. Chung, Adaptive neuro-fuzzy controller for static VAR compensator to damp out wind energy conversion system oscillation, IET Gener. Transm. Distrib. 7 (2) (2013) 200–207.
[29] D.P. Subramanian, R.K. Devi, R. Saravanaselvan, A new algorithm for analysis of SVC's impact on bifurcations, chaos and voltage collapse in power systems, Elsevier Int. J. Electr. Power Energy Syst. 33 (5) (2011) 1194–1202.
[30] H. Amaris, M. Alonso, Coordinated reactive power management in power networks with wind turbines and FACTS devices, Elsevier Energy Convers. Manage. 52 (7) (2011) 2575–2586.
[31] D. Padma Subramanian, R.P. Kumudini Devi, Performance evaluation and comparison of conventional and facts controllers in mitigating chaos driven instabilities, Iran. J. Electr. Comput. Eng. 7 (2) (2008) 140–146.
[32] V.A. Duggirala, V.N.K. Gundavarapu, Improved LVRT for grid connected DFIG using enhanced field oriented control technique with super capacitor as external energy storage system, Eng. Sci. Technol. Int. J. 19 (4) (2016) 1742–1752.
[33] K. Vinothkumar, M.P. Selvan, Novel scheme for enhancement of fault ride-through capability of doubly fed induction generator based wind farms, Elsevier Energy Convers. Manage. 52 (7) (2011) 2651–2658.
[34] O. Anaya-Lara, F.M. Hughes, N. Jenkins, et al., Provision of a synchronising power characteristic on DFIG-based wind farms, IET Gener. Transm. Distrib. 1 (1) (2007) 162–169.
[35] J.M. Carrasco, L.G. Franquelo, J.T. Bialasiewicz, et al., Power-electronic systems for the grid integration of renewable energy sources: a survey, IEEE Trans. Ind. Electron. 53 (4) (2006) 1002–1016.
[36] M. Zellagui, Variable speed of the wind turbine generator with DFIG connected to electric grid, Revue des Energies Renouvelables 11 (3) (2008) 453–464.
[37] L. Aguilar, P. Melin, O. Castillo, Intelligent control of a stepping motor drive using a hybrid neuro-fuzzy ANFIS approach, Elsevier Appl. Soft Comput. 3 (3) (2003) 209–219.
[38] A.G. Aissaoui, A. Tahour, N. Essounbouli, et al., A Fuzzy-PI control to extract an optimal power from wind turbine, Elsevier Energy Convers. Manage. 65 (2013) 688–696.
[39] C.T. Lin, C.G. Lee, Neural-network-based fuzzy logic control and decision system, IEEE Trans. Comput. 40 (12) (1991) 1320–1336.
[40] C.F. Juang, C.T. Lin, An online self-constructing neural fuzzy inference network and its applications, IEEE Trans. Fuzzy Syst. 6 (1) (1998) 12–32.
[41] K. Premkumar, B.V. Manikandan, Bat algorithm optimized fuzzy PD based speed controller for brushless direct current motor, Eng. Sci. Technol. Int. J. 19 (2) (2016) 818–840.
[42] M. Amirrezai, H. Rezaie, G.B. Gharehpetian, H. Rastegar, A new fuzzy-based current control strategy with fixed switching frequency for improving D-STATCOM performance, J. Intell. Fuzzy Syst. 35 (3) (2018) 3285–3294.
[43] A.H. Bonnett, The impact that voltage and frequency variations have on AC induction motor performance and life in accordance with NEMA MG-1 standards, Pulp and Paper, 1999. Industry Technical Conference Record of 1999 Annual (pp. 16-26), IEEE, 1999.